J. Membrane Biol. 54, 165–171 (1980)

The Journal of
Membrane Biology

On the Electrotonic Coupling Mechanism of Crayfish Segmented Axons: Temperature Dependence of Junctional Conductance

F. Ramón and G. Zampighi

Department of Physiology, Duke University Medical Center, Durham, North Carolina 27710

Summary. It is generally accepted that the mechanism for electrotonic coupling involves the presence of hydrophilic channels connecting the cytoplasm of neighboring cells. These channels are presumed to be water filled holes. To test this hypothesis, we measured the temperature dependence of coupling parameters and calculated the specific resistance of junctional synapses of crayfish segmented axons. Results demostrate that: (i) low temperature increases the junctional resistance in a manner that depends on the time course of cooling; (ii) the specific junctional resistance is, at most, 1–20 Ωcm^2. These results are consistent with a hypothesis of cell communication based on hydrophilic channels and suggest the presence of a temperature-dependent component of these channels.

The hypothesis regarding the mechanism of coupling by electrotonic synapses postulates the existence of hydrophilic channels, about 2 nm in diameter and 18 nm in length, connecting the cytoplasm of neighboring cells (Loewenstein, 1966; McNutt & Weinstein, 1970; Makowsky et al., 1977). If this hypothesis is correct, each open channel should be regarded as a water filled pore with a temperature dependence indistinguishable from that of axoplasmic resistance (about 1.3; Huxley, 1959). However, Payton, Bennett and Pappas (1969) reported Q_{10} values of 1/3.1 for the coupling resistance of crayfish electrotonic synapses. Such value of temperature dependence is inconsistent with the current hypothesis.

We have investigated the effects of temperature on electrical parameters of crayfish lateral axons and their electrotonic synapses. Our results, obtained under different conditions than those of Payton et al. (1969), are consistent with a coupling model based on hydrophilic channels filled with a material whose temperature dependence is indistinguishable from that of axoplasm. The data also suggests a component of the coupling mechanism whose temperature dependence is larger than that of axoplasm.

Materials and Methods

Experiments were conducted on lateral axons of the abdominal nerve cord of crayfish *Procambarus clarkii* (obtained from Dahl Biological Supply, Inc., California). Nerve cords were excised from crayfish and placed in a Petri dish containing Van Harreveld (1936) solution at pH 7.4 and osmolarity 460 mOsm. After removal of attached pericordal connective tissue the nerve cord was transfered to an experimental chamber made of Lucite and with a bottom wall 1 mm thick. Temperature was controlled by placing the chamber on a water-cooled thermoelectric assembly (Cambion Electronics). Imposed changes in temperature followed an exponential time course with a time constant of about 2 min. For prolonged changes a half cycle was carried out in steps of 6 °C lasting about 15 min each. Temperature of the bath solution was read, to an accuracy of ±0.25 °C, with an independent thermometer placed near the crayfish nerve cord.

Figure 1 shows a schematic diagram of the experimental arrangement. Propagated action potentials were initiated by stimulating the axons alternatively on each side of the junctional area, with short electrical pulses delivered through small platinum-platinized electrodes, from a Grass Stimulator (S-88). Membrane potentials were recorded with four intracellular microelectrodes placed within a maximum distance of about 500 µm from the septal region. A switching device allowed us to choose any internal microelectrode to deliver current pulses from a stimulator (Tektronix, 160 series) with a series resistance of 250 or 500 MΩ.

The temperature dependence (Q_{10}) of parameters measured was calculated with the relationship

$$V_1 = V_o Q_{10}^{(T_i - T_o)/10} \quad (1)$$

where V_o is the parameter value at the reference temperature (T_o = 15 °C). According to this definition, Q_{10} is greater than unity when values of measured parameters increase as temperature increases, and smaller than unity (expressed as a fractional number) when measured parameters decrease as temperature increases.

0022-2631/80/0054-0165 $01.40

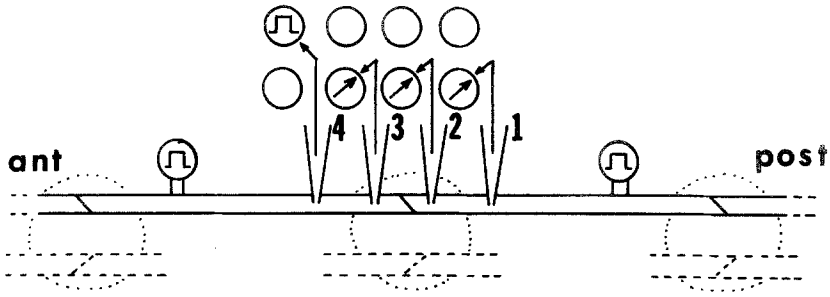

Fig. 1. Schematic diagram of the experimental setup. Four microelectrodes, two at each side of the septal region, are introduced in the lateral axon at the 3rd abdominal ganglion. Each one of the microelectrodes could be selected to inject current or to record membrane voltage. Two pairs of external electrodes placed on the axon, far from the ganglion, are used to elicit propagated action potentials.

Results

A. Temperature Effects

1. Propagated action potentials. Figure 2*A* shows data obtained from an experiment performed after the nerve cord had been excised and placed in van Harreveld solution at 6 °C for about 30 min. The pre-junctional action potential amplitude (filled circles) shows an average value of about 102 mV in the range 6–23 °C, hence it decays to 82 mV at 32 °C. The amplitude of post-junctional action potentials (open circles) is smaller at low temperature, reaches a maximum of about 102 mV around 15 °C, and then it decays as temperature is further increased. Figure 2*B* shows values of resting potential recorded by the same pre- and post-junctional electrodes. These data points were fitted, at middle range (10–25 °C), by a straight line with a slope of −0.45 mV/°C (Q_{10} = 1.07).

Table 1 shows values of minimum and maximum speed of propagation of action potentials obtained at 6 and 31 °C, respectively. The speed of propagation of action potentials was calculated by measuring the distance between microelectrodes 1–2, 2–3, or 3–4 (*see* Fig. 1), and dividing by the time interval required to reach half maximum amplitude of corresponding action potentials. These data points were fit by straight lines whose slopes are given in units of m/sec/°C. Included in Table 1 is the calculated Q_{10}.

2. Coupling parameters. We measured the effect of temperature on membrane voltage changes, both transient and steady state, that arise when current is injected on one side of the junctional area between two axons. Figure 3*A* shows that the magnitude of these voltage changes is nearly independent of temperature in the range 6–27 °C. The abrupt and partial uncoupling at 29 °C seen in Fig. 3*A* does not occur in all preparations and frequently uncoupling is gradual. Data points fall along straight lines with slopes of 0.05 and 0.07 mV/°C (Q_{10} = 1.08 and 1.12) for pre- and post-junctional recordings, respectively. The time

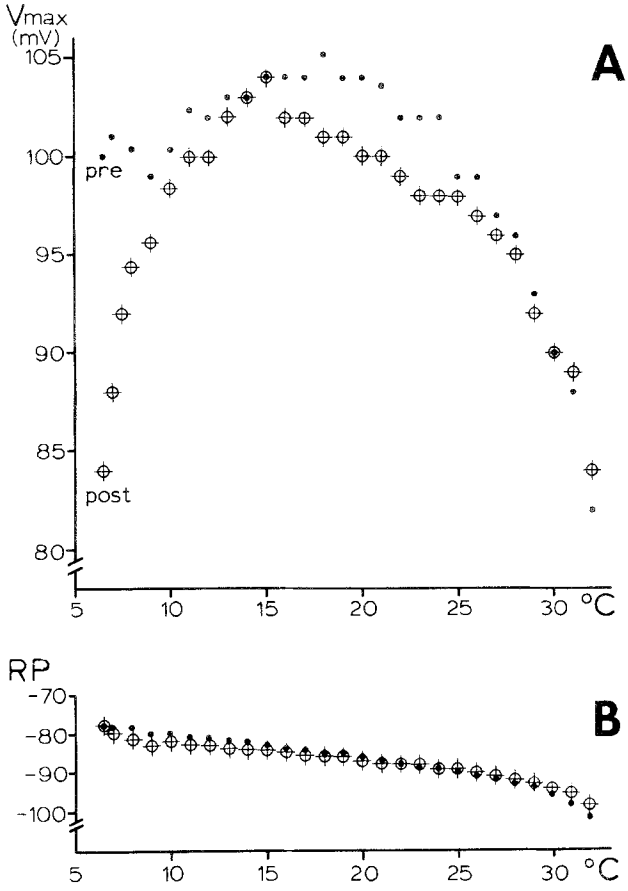

Fig. 2. Maximum amplitude of action potentials, propagating from anterior to posterior axon segments, and resting potentials as function of temperature. (*A*): Amplitude of pre- (filled circles) and post-junctional (empty circles with a + sign) action potentials. In this experiment there were two post-junctional microelectrode recordings and empty circles with a + sign are average of measurements by these two microelectrodes. (*B*): Values of resting potentials for the same microelectrode recordings are shown. This experiment was conducted after the nerve cord had been placed in cold (6 °C) solution for about 30 min.

constants of these voltage changes are also slightly affected by temperature (Fig. 3*B*). Straight lines that fit these data points have slopes of −0.024 and −0.023 msec/°C (Q_{10} = 1/1.17 and 1/1.23) for pre- and post-junctional recordings, respectively. The ra-

Table 1. Speed of propagation of action potentials at septal and two paraseptal axon regions as function of temperature[a]

	Anterior		Septal		Posterior	
	min 6 °C	max 31 °C	min 6 °C	max 31 °C	min 6 °C	max 31 °C
$A \rightarrow P$ (m/sec)	3.60	8.50	1.20	9.35	4.20	21.50
slope (m/sec/°C)	0.17		0.28		0.62	
(Q-10)	1.67±	0.20	1.67±	0.18	1.41±	0.15
$P \rightarrow A$ (m/sec)	2.40	10.90	1.80	9.05	2.50	17.4
slope (m/sec/°C)	0.30		0.26		0.53	
(Q-10)	1.54±	0.23	1.70±	0.19	1.26±	0.10

[a] The table includes values for the two extremes in the temperature range measured. *A* stands for anterior, *P* for posterior, axon segment.

tio of these time constants has been plotted in Fig. 3 *C*. In spite of scatter of the data, the relationship is nevertheless best described by a straight line (slope of −0.001 msec/°C). Thus, temperature dependence of steady-state, and time constant, values of voltage changes produced in response to intracellular current pulses is small. Furthermore, the near temperature independence of the ratio of post- to pre-junctional time contants suggests that these effects are predominantly due to surface and not to junctional membranes.

The data presented above, with a small temperature dependence of coupling, suggests purely passive mechanisms. However, the possibility of some energy-dependent process at the electrotonic coupling mechanism becomes plausible again after comparing our data with the experiments of Payton et al. (1969). These authors showed a high temperature dependence of coupling resistance of crayfish lateral axons ($Q_{10} = 1/3.1$) when the temperature was changed rapidly.

To directly compare our results and those of Payton et al. (1969) we have replotted in Fig. 4 data from their Fig. 3 (open circles) and calculations from the same data shown in our Fig. 3*A* (filled circles). We also cooled our preparation faster (about 8 min) than previously to facilitate the comparisons. Data points (stars) from these experiments show an increase in junctional resistance. Furthermore, if after slow cooling (filled circles) the axons are allowed to stay at about 5 °C for more than 30 min, the junctional resistance increases until it reaches values close to $10 \times 10^5\ \Omega$. After uncoupling and recoupling has been obtained a first time by lowering and raising the temperature, subsequent exposure to low temperatures produces uncoupling at progressively higher temperatures.

When rapid and slow cooling experiments are performed on the same axon, results show variability. In four out of six experiments we obtained results similar to those described above. In the other two experiments junctional resistance increased as temperature was lowered, irrespective of rate, in a way that resembled results from rapid cooling. This variability seems independent of the sequence in which experiments are performed.

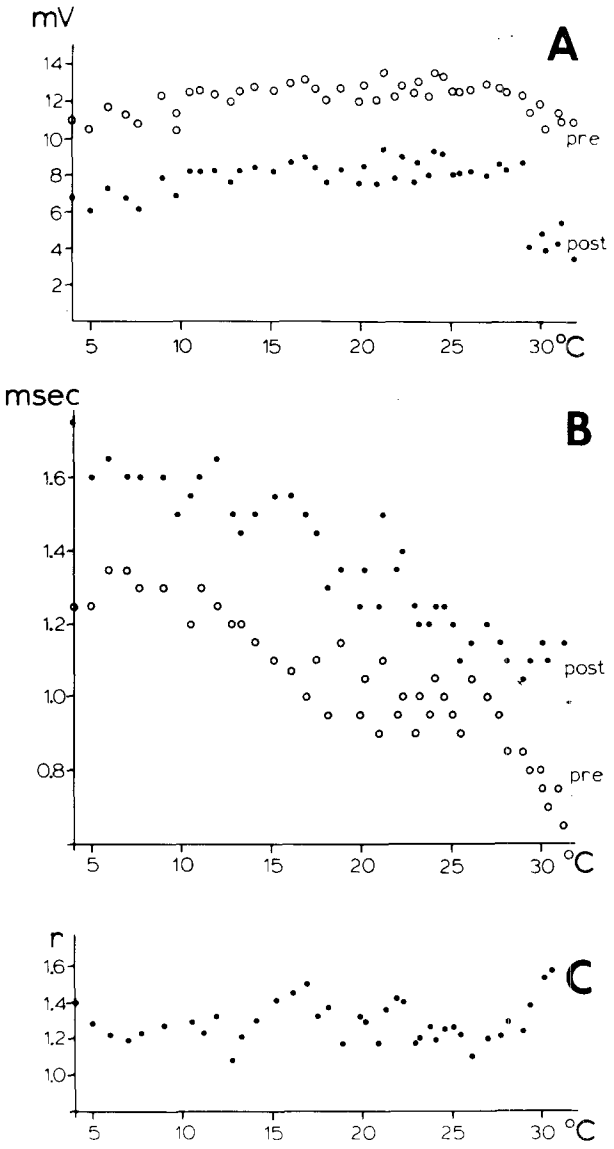

Fig. 3. Membrane voltage changes produced by intracellularly injected current pulses as function of temperature. (*A*): Steady-state values of pre- (empty circles) and post-junctional (filled circles) recordings. (*B*): Time constants (1/*e*) of membrane voltage changes plotted in *A*. (*C*): The ratio of these post- to pre-junctional time constants.

3. Junctional conductance. Three experiments were conducted in which the bath temperature was changed

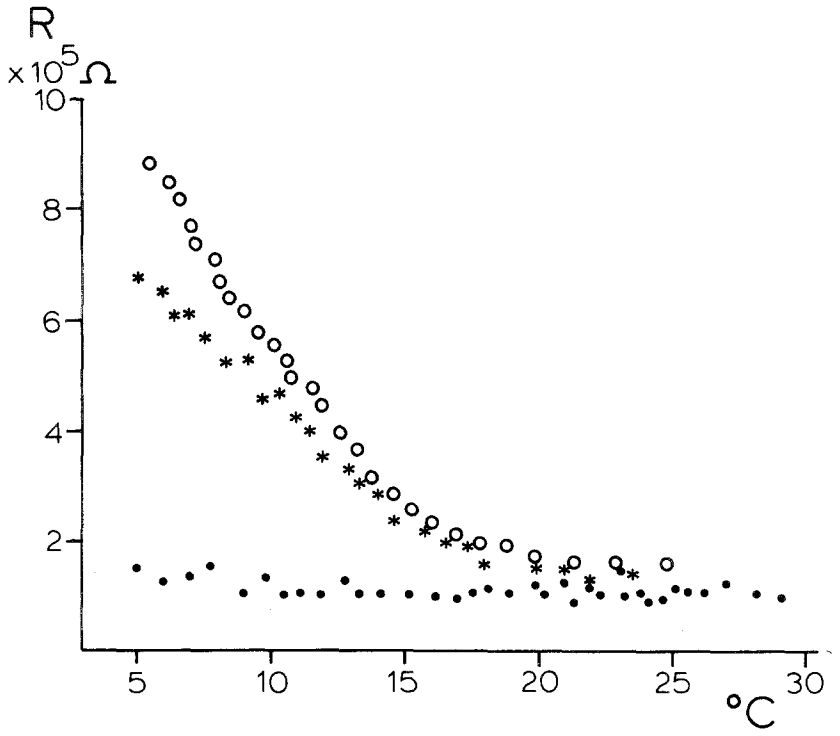

Fig. 4. Septal resistance of crayfish axons as a function of temperature. Empty circles are data replotted from an experiment by Payton et al. (1969; their Fig. 3). Filled circles were calculated from our data shown in Fig. 3*A*, obtained by slow cooling, and stars are data points obtained by an intermediate rate of cooling.

from 21 to 2 °C in about 30 min and maintained at 2 °C for as long as required to produce uncoupling of the axon segments. Junctional conductance values were computed from the current voltage relationships resulting from injecting slow (about 0.1 μA/sec) ramps of current through one of the microelectrodes. Figure 5 shows results from one of these experiments. Junctional conductance (open circles) decreased as the nerve cord remains at low temperature. The filled circle indicates the value of junctional conductance at which the action potential stopped propagating across the junctional region. The right-most open circle is the theoretical limit of junctional conductance calculated for two closely apposed, but uncoupled, axons. Propagated action potentials recorded by two microelectrodes at each side of the junctional area demonstrate, first, the slowing of the speed of propagation (*2*), and then blocking at the junctional region (*3*). These effects are reversible, and rewarming to 21 °C restores junctional conductance to nearly control values.

B. Junctional Resistivity

The junctional resistance was measured in experiments in which four microelectrodes, two at each side of the septal area, impaled the axons (Fig. 1). Square pulses of current were injected through one microelectrode while the other three made simultaneous voltage recordings, with all four microelectrodes being alternatively selected to inject current. Data from one axon segment was obtained by the procedure outlined below and similar steps were followed to calculate data for the other axon. The length constant (λ) at both sides of the septum was calculated from the four sets of measurements obtained as each microelectrode was used to inject current. For these calculations we took the membrane potential as a declining exponential on both sides of the injecting electrode. This approach is justified by anatomical studies demonstrating that the axons do not terminate at the septum (Johnson, 1924).

$$\lambda_{3,4} = \Delta x_{3,4} / (\ln V_3^1 - \ln V_4^1) \tag{2}$$

here Δx is the distance between electrodes, subscripts indicate the recording electrode, and superscripts the current injecting electrode. All four microelectrodes were used to inject current and four values of λ were calculated, two for each axon segment. Table 2 shows the mean values of these calculations.

Using those values of length constant, we obtained the voltage amplitude at a current injecting point (V_4^4, Eq. (3)) and the membrane voltage at the corresponding side of the septum (V_{s3}^4, Eq. (4)). With similar equations for the other axon segment, it is then possible to obtain the voltage drop across the septal area (ΔV_s, Eq. (5)).

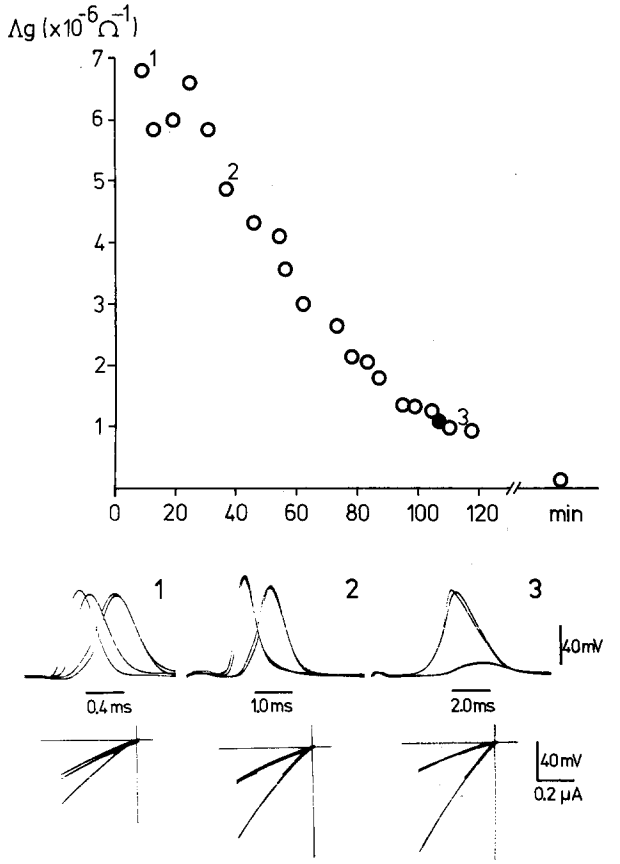

Fig. 5. Junctional conductance as a function of time when the temperature is changed from 21 to 2 °C in the first 30 min. The right-most point corresponds to the theoretical limit of junctional conductance, calculated for two closely apposed membranes ($R_m = 5\,k\Omega cm^2$). The filled circle signals time at which action potential propagation stopped at the junctional region. The middle part of the figure shows action potentials recorded by two microelectrodes at each side of the junction at the times specified by the corresponding number in the plot of junctional conductance. Note that the time scale is different for each group of action potentials. The lowest three records are current-voltage relationships recorded in response to intracellular injection of ramps of current. These ramps had a slope of 0.1 μA/sec. The time of their recording does not correspond with those of action potentials.

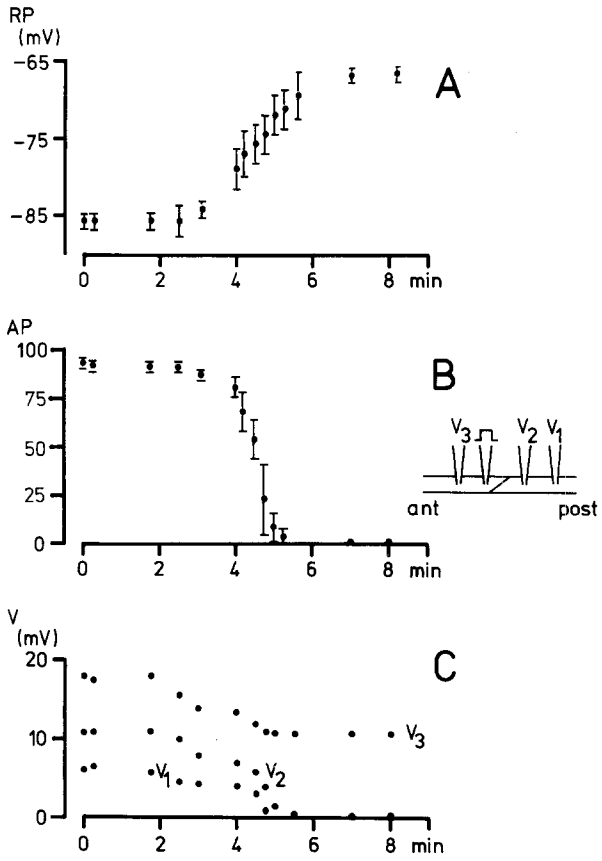

Fig. 6. Axon parameters during fixation of the crayfish nerve cord with glutaraldehyde (3 %). Time 0 corresponds to the moment at which the drug begins to substitute the bath solution. (*A*): Mean resting potential (±SD) measured by three microelectrodes (*see* diagram). (*B*): Mean amplitude (±SD) of the action potential measured by the same microelectrodes. (*C*): Steady-state amplitude of pre- and post-junctional voltage changes (*see* text for further discussion).

Table 2. Cable parameters of crayfish lateral axons

	Anterior	Posterior
Input resistance, *Ro* (kΩ)	46.83±3.52	56.53±2.94
Length constant, λ (mm)	0.80±0.12	1.42±0.32
Septal resistivity, *Rs* (Ωcm^2)	1.20±0.30	0.43±0.09

$$V_4^4 = V_3^4 \exp(\Delta x_{3,4}/\lambda_{3,4}) \quad (3)$$

$$V_{s3}^4 = V_3^4 \exp(-\Delta x_{3,s}/\lambda_{3,4}) \quad (4)$$

$$\Delta V_s^4 = V_{s3}^4 - V_{s2}^4. \quad (5)$$

The voltage drop recorded by two ipsi-septal electrodes and the internal resistance (r_i, Ω/cm) between these two regions (with $R_i = 100\,\Omega cm$; Watanabe & Grundfest, 1961) yielded an aproximate value for the axial current (i_{s4}, Eq. (6)) reaching the septum, and the septal resistivity (R_s, Eq. (7)).

$$i_{s4} = (V_3^4 - V_{s3}^4)/r_i \Delta x_{s3} \quad (6)$$

$$R_s^4 = A \Delta V_s / i_{s4}. \quad (7)$$

For these calculations the corrected synaptic area (*A*) was obtained as described in Discussion.

Table 2 shows the results of those measurements and calculations obtained from 6 different experiments at a temperature of about 15 °C.

C. Effect of Glutaraldehyde

A drug currently used in electromicroscopy for fixation of biological preparations, glutaraldehyde, produces cell uncoupling (Bennett et al., 1972). Figure 6

Table 3. Membrane and septal resistances ($\times 10^3\,\Omega$) before and after fixation with glutaraldehyde

	Anterior	Septal	Posterior
Normal	85.2±4.0	141.9± 30.0	92.6±5.0
Glutaraldehyde	65.5±5.0	2750.0±214.0	39.2±2.0

shows a plot of some axon parameters as function of time after glutaraldehyde (3 %) begins to replace the bath solution. Figure 6*A* shows mean values of resting potential recorded by three microelectrodes (inset, Fig. 6). As glutaraldehyde reaches the nerve cord, membrane potentials decrease by about 18 mV from resting values of −85 mV. Figure 6*B* shows maximum amplitude of propagated action potentials being progressively decreased by glutaraldehyde. Figure 6*C* shows steady-state amplitudes of membrane potential changes produced in response to injection of current pulses. These amplitudes decrease in all three recordings; however, while post-septal voltages (V_1 and V_2) are completely abolished, the pre-septal potential (V_3) is only reduced.

Measurements of potential changes before and after application of glutaraldehyde to nerve cords could also be used to obtain an independent value of the junctional resistance. Values for surface and septal membrane resistances were obtained by a procedure described by Watanabe and Grundfest (1961). This method, derived from analysis of the equivalent circuit for septated axons, consists in treating the junctional axon region as a π resistor network. Injection of square pulses of current at both sides of the transversal section of the network (the junctional resistance), and voltage recordings at both axons, allows the utilization of the equations derived by Watanabe and Grundfest (1961, p. 284; *see also* Asada & Bennett, 1971). Results from these experiments are summarized in Table 3.

Table 3 shows that pre- and post-septal membrane resistances *decrease* after fixation with glutaraldehyde; however, the junctional resistance *increases* by a factor of about 20. Since glutaraldehyde produced cell uncoupling, as we demonstrated previously (Fig. 6), values obtained after this drug reflect that resistance between uncoupled cells. Thus a septal resistance of 2750 kΩ, and a septal (not only junctional) membrane area of 14,130 μm^2 (*see* Discussion), allow us to calculate a membrane resistivity of 400 $\Omega\,cm^2$, slightly below the normal nonjunctional membrane resistivity (Cole, 1968). From the ratio of junctional resistances before and after glutaraldehyde (19.3), the normal septal resistivity can be calculated to be about 20 Ωcm^2.

Alternatively, we can calculate the junctional resistivity from values of junctional resistance obtained before glutaraldehyde fixation (Table 3). These values, and our estimate of septal synaptic area (about 500 μm^2; *see* below), yield a junctional membrane resistivity of about 1 Ωcm^2 in the coupled state.

Discussion

1. Effects of Temperature

Data concerning the effect of temperature on axon and junctional parameters shows three clearly defined regions. At low temperatures (<10 °C) there is an increase in junctional resistance that can be observed as a partial block of propagated action potentials at post-junctional regions (Fig. 2*A*). At high temperatures (>25 °C) there is also a decrease in aplitude of pre- and post-junctional action potentials (Fig. 2*A*) and of post-junctional voltage changes (Fig. 3*A*). In the middle range (10–20 °C) the amplitude of action potentials remains constant (Fig. 2*A*), and pre- and post-junctional voltage changes produced in response to injection of current pulses (Fig. 3*A*) are similarly unaffected. In this middle range, values for the Q_{10} of these voltage changes (1.1–1.2) are comparable to those obtained for junctional resistance (1.17; Fig. 4, filled circles) and also those calculated for axoplasmic resistance (1.3; Huxley, 1959).

Data shown in Table 1 demonstrate that the speed of propagation of action potentials has similar temperature dependence at both sides of the junctional region. Thus, the smaller amplitude of action potentials recorded at post-junctional axon segments at low temperature (Figs. 2*A* and 5) is not due to differences in the axonal membranes and it probably depends on a partial block at the junction. Similar data shown in Fig. 5 demonstrates that variability in coupling resistance does not necessarily reflect variability in propagation of action potentials across the septum, as these propagate up until the junctional conductance decreases below $1 \times 10^{-6}\,\Omega^{-1}$.

Increase in coupling resistance at low temperatures suggests the presence of an energy-dependent component of the electrotonic synapse. This observation agrees with data about the uncoupling effect of metabolic blockers (DNP) and prolonged low temperature on other low resistance junctions (Politoff, Socolar & Loewenstein, 1969). These results have been interpreted as due to changes in cytoplasmic calcium as a result of metabolic inhibition, and a similar explanation could account for our results at low temperatures. In contrast, effects of high temperature are probably not predominantly on junctional synapses, since similar effects can be observed in pre- and post-junctional propagated action potentials, al-

though not necessarily on voltage changes in response to current pulses.

Variability in temperature dependence of junctional resistance when performing rapid and slow cooling experiments on the same axon cannot be easily explained. Lateral axons might undergo changes in their metabolic state that could be related to alteration in the cytoplasmic calcium concentration (Rose & Loewenstein, 1976) or in intracellular pH (Turin & Warner, 1977). Electrotonic uncoupling after axons are allowed to stay in cold solution for long periods of time could also be due to the same mechanisms. However, it is worthwhile to note that under these conditions we have observed widening of the space between contiguous axons, similar to that observed under other conditions (Pappas, Asada & Bennett, 1971).

2. *Junctional Resistivity*

Values for specific septal resistance calculated in our experiments agree well with those reported for crayfish axons (Watanabe & Grundfest, 1961) and other electrotonic synapses (Furshpan & Potter, 1968; Brink & Barr, 1977). However, as already indicated, septal area is not a proper measure of junctional area. Anatomical data clearly shows that the whole septum is not covered by synaptic contacts (Hama, 1961; Zampighi, Ramón & Duran, 1978) and better estimations of the synaptic membrane area can be made. We estimated about 20 "windows" at a given septal wall, a number that comes about from measurements of the average spacing between windows on microphotographs of thin sections of the septal area. At each one of these windows an axon sends a semicircular projection of about 4 μm in diameter to its neighbor. If these projections were spherical and half of that sphere were covered by synaptic regions, the synaptic area of those 20 projections would be $20 \times 25\,\mu m^2 = 500\,\mu m^2$. A correction factor of about 28 was introduced, yielding values for junctional resistivity of about 0.4–1.2 Ωcm^2. Such small values for specific resitance of electrotonic junctions have also been reported in other preparations (*see* Discussion in Brink & Barr, 1977).

In summary, the effects of temperature on parameters of action potentials and coupling mechanism are compatible with the presence of cytoplasmic channels of communication between cells. The data also suggests that a component of these channels is energy dependent.

We are greatly indebted to Drs. S. Simon, J.E. Hall, R. Joyner and J.W. Moore for many useful discussions on our data and suggestions for improving the original manuscript. Dr. L. Barr kindly sent us a previously unpublished manuscript and Dr. N. Stockbridge wrote the text handling computer program that made possible the multiple drafts of this paper. We also appreciate the invaluable assistance of Mr. E. Harris and Mrs. D. Cruthfield.

This work was supported by a Grant from the North Carolina United Community Services and NIH Grants HL 22767 and NS 03437.

References

Asada, Y., Bennett, M.V.L. 1971. Experimental alteration of coupling resistance at an electrotonic synapse. *J. Cell Biol.* **49**:159

Bennett, M.V.L., Spira, M.E., Pappas, G.D. 1972. Properties of electrotonic junctions between embryonic cells of *Fundulus*. *Dev. Biol.* **29**:419

Brink, P., Barr, L. 1977. The resistance of the septum of the median giant axon of earthworm. *J. Gen. Physiol.* **69**:517

Cole, K.S. 1968. Membranes, Ions and Impulses. University of California Press. Berkeley-Los Angeles

Furshpan, E.J., Potter, D.D. 1968. Low resistance junctions between cells in embryos and tissue culture. *In:* Current Topics in Developmental Biology. A.A. Moscona and A. Monroy, editors. Vol. 3, pp. 95–127. Academic Press, New York

Hama, K. 1961. Some observations on the fine structure of the giant fibers of crayfishes (*Cambarus virilus* and *Cambarus clarkii*) with special reference to the submicroscopic organization of the synapses. *Anat. Rec.* **141**:275

Huxley, A.F. 1959. Ion movement during nerve activity. *Ann. N.Y. Acad. Sci.* **81**:221

Johnson, G.E. 1924. Giant nerve fibers in crustaceans with special reference to *Cambarus* and *Palaemonetes*. *J. Comp. Neurol.* **36**:323

Loewenstein, W.R. 1966. Permeability of cell junctions. *Ann. N.Y. Acad. Sci.* **137**:441

Makowsky, L., Caspar, L.D., Phillips, W.C., Goodenough, D.A. 1977. Gap-junctions structures. II. Analysis of the X-ray diffraction data. *J. Cell Biol.* **74**:629

McNutt, N.S., Weinstein, R.S. 1970. The ultrastructure of the nexus. A correlated thin-section and freeze-cleave study. *J. Cell Biol.* **45**:666

Pappas, G.D., Asada, Y., Bennett, M.V.L. 1971. Morphological correlates of increased coupling resistance at an electrotonic synapse. *J. Cell Biol.* **49**:173

Payton, B.W., Bennett, M.V.L., Pappas, G.D. 1969. Temperature dependence of resistance at an electronic synapse. *Science* **165**:594

Politoff, A.L., Socolar, S.J., Loewenstein, W.R. 1969. Permeability of a cell membrane junction. Dependance on energy metabolism. *J. Gen. Physiol.* **53**:498

Rose, B., Loewenstein, W.R. 1976. Permeability of a cell junction and the local cytoplasmic free ionized calcium concentration. A study with aequorin. *J. Membrane Biol.* **28**:87

Turin, L., Warner, A. 1977. Carbon dioxide reversibly abolishes ionic communication between cells of early amphibian embryo. *Nature (London)* **270**:56

Van Harreveld, A. 1936. A physiological solution for fresh water crustaceans. *Proc. Soc. Exp. Biol. Med.* **34**:428

Watanabe, A., Grundfest, H. 1961. Impulse propagation at the septal and commissural junctions of crayfish lateral giant axons. *J. Gen. Physiol.* **45**:267

Zampighi, G., Ramón, F., Durán, W. 1978. Fine structure of the lateral giant axons electrotonic synapse of crayfish (*Procambarus clarkii*). *Tissue Cell* **10**:413

Received 6 February 1980